ARL-TR-10122 • July 2025

Determining Ground Vehicle Direction of Travel from a Magnetic Anomaly Time Series

by Timothy M. Pritchett

DISTRIBUTION STATEMENT A. Approved for public release: distribution unlimited.

NOTICES

Disclaimers

The findings in this report are not to be construed as an official Department of the Army position unless so designated by other authorized documents.

Citation of manufacturer's or trade names does not constitute an official endorsement or approval of the use thereof.

Destroy this report when it is no longer needed. Do not return it to the originator.

ARL-TR-10122 ● JULY 2025

Determining Ground Vehicle Direction of Travel from a Magnetic Anomaly Time Series

Timothy M. Pritchett
DEVCOM Army Research Laboratory

DISTRIBUTION STATEMENT A. Approved for public release: distribution unlimited.

REPORT DOCUMENTATION PAGE

1. REPORT DATE	2. REPORT TYPE	3. DATES COVERED START DATE	3. DATES COVERED END DATE
July 2025	Technical Report	12/01/2024	3/1/2025

4. TITLE AND SUBTITLE
Determining Ground Vehicle Direction of Travel from a Magnetic Anomaly Time Series

5a. CONTRACT NUMBER	5b. GRANT NUMBER	5c. PROGRAM ELEMENT NUMBER
5d. PROJECT NUMBER	**5e. TASK NUMBER**	**5f. WORK UNIT NUMBER**

6. AUTHOR(S)
Timothy M. Pritchett

7. PERFORMING ORGANIZATION NAME(S) AND ADDRESS(ES)	8. PERFORMING ORGANIZATION REPORT NUMBER
DEVCOM Army Research Laboratory ATTN: FCDD-RLA-LB Adelphi, MD 20783	ARL-TR-10122

9. SPONSORING/MONITORING AGENCY NAME(S) AND ADDRESS(ES)	10. SPONSOR/MONITOR'S ACRONYM(S)	11. SPONSOR/MONITOR'S REPORT NUMBER(S)

12. DISTRIBUTION/AVAILABILITY STATEMENT
DISTRIBUTION STATEMENT A. Approved for public release: distribution unlimited.

13. SUPPLEMENTARY NOTES
ORCID: Timothy M. Pritchett, 0000-0002-8024-0850

14. ABSTRACT
Estimates of two parameters related to the movement of a ground vehicle may be obtained from a time series of the magnetic anomaly resulting from the vehicle, recorded by a single three-axis magnetometer: 1) the ratio v/d_{CPA} of the vehicle speed v to the distance d_{CPA} of closest approach of the vehicle to the magnetometer; and 2) direction of vehicle travel (azimuth angle α) modulo 180°. Using data from only a single magnetometer, one cannot determine in which of two diametrically opposed directions the vehicle is traveling; that is, azimuths of α and $\alpha + \pi$ are indistinguishable. This ambiguity is easily removed using data from a second sensor, either a nearby magnetometer or an acoustic sensor, possibly collocated with the first magnetometer. When d_{CPA} is at least several vehicle lengths, the determination of v/d_{CPA} is extremely reliable and can be used to independently verify estimates of speed or closest approach distance obtained from acoustic sensor data. This lower bound on d_{CPA} establishes a window over which parameter estimates can be successfully extracted from time series data. For a low size, weight, and power magnetometer with limited sensitivity, this window may be inconveniently narrow.

15. SUBJECT TERMS
magnetic anomaly detection, magnetic signature, magnetic field, three-axis magnetometer, direction of travel, Electromagnetic Spectrum Sciences

16. SECURITY CLASSIFICATION OF: a. REPORT	b. ABSTRACT	C. THIS PAGE	17. LIMITATION OF ABSTRACT	18. NUMBER OF PAGES
UNCLASSIFIED	UNCLASSIFIED	UNCLASSIFIED	UU	25

19a. NAME OF RESPONSIBLE PERSON	19b. PHONE NUMBER *(Include area code)*
Timothy M. Pritchett	(520) 691-6327

STANDARD FORM 298 (REV. 5/2020)
Prescribed by ANSI Std. Z39.18

Contents

List of Figures

List of Tables

1. Introduction

Like virtually all objects, a ground vehicle produces a distortion in the local magnetic field. This distortion arises from the transient magnetic moments that the ambient field of the earth induces in all materials of non-unit relative permeability, as well as the more persistent moments that the ambient terrestrial field induces in ferromagnetic materials. At standoff distances of approximately one vehicle length, the transient ("induced") and more enduring ("remnant," often referred to as "permanent") moments associated with a vehicle are well approximated by a collection of point dipoles,[1–4] and at even greater standoff distances (multiple vehicle lengths), by a single point dipole.

One can think of the total magnetic moment associated with a piece of ferromagnetic material—and, in particular, with a ferromagnetic component of a vehicle, such as the engine, chassis, or, in the case of many tactical vehicles, armor—as consisting of an induced moment that is oriented in the direction of the local ambient field and a remnant moment whose spatial orientation reflects the vehicle's prior history of orientation with respect to the ambient field, its specific manufacturing history, and other factors. The direction of the remnant moment is thus not known a priori. While it will—particularly if the ferromagnetic material is subject to mechanical stress—eventually align itself with the local ambient field as those magnetic domains whose spins are aligned with external field increase in size at the expense of the others, the time scale for this realignment is relatively long.

In the case of a ground vehicle, which is virtually always oriented upright on a surface that is approximately horizontal, it is reasonable to assume that the components of the vehicle's induced and remnant magnetic moments along a vertical axis fixed in the vehicle are constant in time, as is their sum, the vertical component of the total magnetic moment of the vehicle. (Here we tacitly assume that the vehicle has not recently moved from a location on the earth's surface where the ambient magnetic field is significantly different, and that the configuration of its ferromagnetic components has not changed, as would occur, for instance, if a tank gun were raised or lowered.) As the vehicle moves and its orientation relative to the terrestrial field changes, the components of the induced moment along horizontal axes fixed in the vehicle change in time essentially instantaneously. In contrast, components of the remnant moment change so slowly that the alteration is negligible on the time scale of any series of practical measurements, and the remnant moment can be considered constant and fixed in the vehicle. However, the direction of the horizontal component of the remnant moment is in general unknown and so, too, is the magnitude and direction of the horizontal component of the sum of the remnant and induced moments of the vehicle.

In this report, we describe a method for extracting two parameters related to the movement of a ground vehicle from a time series of the magnetic anomaly resulting from the vehicle, obtained from a single vector magnetometer. From the vertical (z-) component of the magnetic anomaly, we obtain an estimate of v/d_{CPA}, the ratio of the vehicle speed, v, to d_{CPA}, the distance between the vehicle and the magnetometer at their closest point of approach (CPA). From the components of the anomaly in the horizontal (xy-) plane, we determine the direction of vehicle travel (azimuth angle α) modulo 180°. These estimates are valid as long as d_{CPA} is at least several vehicle lengths.

This report is organized as follows. In Section 2, we specify the geometry of the encounter between the magnetic field sensor and the passing vehicle (magnetic source). In Section 3, we describe a simple analytic model that represents a ground vehicle as a collection of point dipoles, and we verify that this model reduces at large distance to a model involving only a single point dipole, the dipole moment of which is given by the vector sum of the individual point dipoles in the original multiple-dipole model. We then express the magnetic anomaly obtained from the asymptotic single-dipole model in terms of the representation developed by J.E. Anderson for a point dipole in uniform, linear motion.[5,6] In Section 4, we describe a procedure for estimating the ratio v/d_{CPA} and the azimuth angle α from time series data obtained from a single vector magnetometer, and in Section 5 we present representative results obtained using simulated magnetic anomaly data with known values of these quantities, and we consider the impact of random noise on the parameter estimates obtained from the model. In Section 6, we discuss the implications of these methods for near-future Army sensing applications.

2. Geometry of the Encounter between Sensor and Magnetic Source

In this report, we model the magnetic anomaly that arises from the straight-line motion of a vehicle in the ambient terrestrial field and is registered as a function of time by a sensor at a nearby observation point. To enable our discussion, we first specify the geometric relationship between the sensor and the vehicle (magnetic source).

We consider the two reference frames illustrated in Figure 1. Frame S is at rest with respect to the earth and thus also to a fixed sensor located at position $\vec{x}_0$. Frame S' is at rest with respect to the vehicle and moves with it at velocity $\vec{v}$ relative to S. We take the corresponding Cartesian axes of the two frames to be parallel, with the x- and x'-axes directed due east, the y- and y'-axes directed due north, and the z- and z'-axes directed vertically upward.

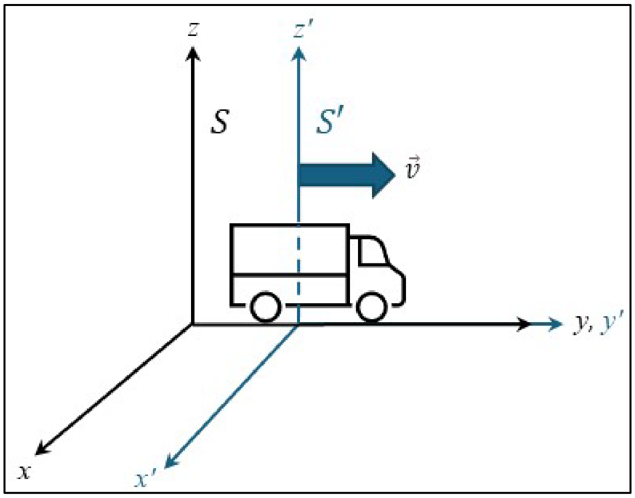

Figure 1. Frames of reference used to describe the encounter between a passing vehicle (magnetic source) and a stationary sensor. Reference frame S is at rest with respect to the earth and sensor, whereas S' moves with the vehicle at velocity $\vec{v}$ relative to S. We take the origin of S' to lie at the point on the ground directly below the center of the vehicle ("epicenter").

We choose time $t = 0$ to be the instant at which the origins of the two frames coincide. With this choice, the Galilean transformation relating $\vec{x}$, the coordinates in S of a given point, and $\vec{x}'$, its coordinates in S', takes the following simple form:

$$\vec{x}' = \vec{x} - \vec{v}t \; . \tag{1}$$

We also choose $t_{CPA} = 0$, where t_{CPA} is the time at which the vehicle reaches its CPA to the sensor; frames S and S' thus coincide at the instant that the CPA is reached. Finally, we locate the origin of S' at the point in the horizontal plane of the sensor that lies directly below the center of the vehicle. Taking our cue from the terminology used in seismology, we will refer to this point as the epicenter of the vehicle. Since the sensor will virtually always be situated on the ground, this means that $z = z' = 0$ corresponds to ground level in both frames, the most natural choice and the choice illustrated in Figure 1. From these choices, it follows that $|\vec{x}_0| = d_{CPA}$, where d_{CPA} is the distance separating the sensor and the vehicle at their CPA.

The direction of the velocity is specified by the azimuth angle α, which by convention is measured eastward from true north (or clockwise from the y-axis, as shown in Figure 2). The truck in Figure 1 thus has an azimuth of zero. The unit vector in the direction of the velocity of the vehicle, $\hat{v} = \vec{v}/v$, is related to the azimuth by

$$\hat{v} = \hat{x} \sin \alpha + \hat{y} \cos \alpha \; . \tag{2}$$

Observe that

$$\hat{v}(\alpha + \pi) = -\hat{v}(\alpha) \; . \tag{3}$$

Figure 2 depicts the situation at $t = t_{CPA} = 0$, the instant at which the axes of S and S' coincide and the center of the vehicle is at its CPA to the sensor.

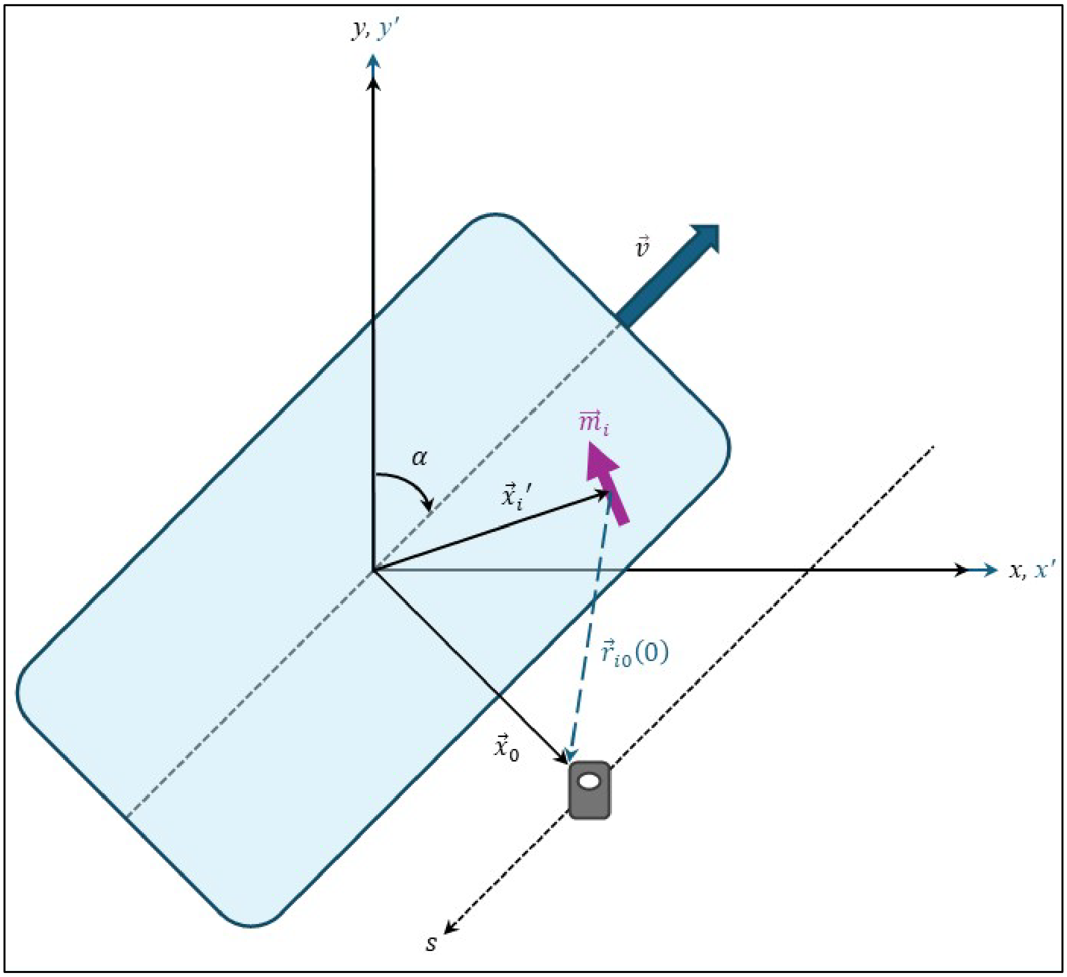

Figure 2. Top view of the sensor and passing vehicle (magnetic source) at time $t = 0$, the moment of closest approach. The *z*-axis points out of the page. Vectors $\vec{r}_{i0}(0)$ and $\vec{x}_i{}'$, which have a nonzero *z*-component, are represented by their projections on the *xy*-plane.

The velocity $\vec{v}$ of the vehicle and the position vector $\vec{x}_0$ of the sensor are mutually perpendicular in S. This suggests that we define the unit vectors

$$\hat{x}_0 = \vec{x}_0 / d_{CPA} = \hat{x}\cos\alpha - \hat{y}\sin\alpha \tag{4}$$

and

$$\hat{u} = \hat{z} \times \hat{x}_0 \, . \tag{5}$$

By construction, the unit vectors $(\hat{x}_0, \hat{u}, \hat{z})$ form a right-hand triple. They serve as basis vectors for a particularly convenient coordinate system in which the sensor is at rest. We define the sign σ of the velocity with respect to $\hat{u}$:

$$\sigma = \hat{v} \cdot \hat{u} = \hat{v} \cdot (\hat{z} \times \hat{x}_0) = \hat{z} \cdot (\hat{x}_0 \times \hat{v}) \, , \tag{6}$$

so that

$$\vec{v} = \sigma\, v\, \hat{u}\,. \tag{7}$$

The last equality in Equation 6 follows from the circular shift property of the scalar triple product.

The quantity σ defined in Equation 6 has several equivalent interpretations. For instance, it indicates whether the unit vectors $(\hat{x}_0, \hat{v}, \hat{z})$ form a right-hand triple $(\sigma = +1)$ or a left-hand triple $(\sigma = -1)$. Perhaps more germane to our discussion here, it differentiates between the two possible positions $\vec{x}_0$ of the sensor for a given $\hat{v}$ and d_{CPA}, and it is related to the 180° ambiguity in the estimate of the azimuth angle.[1]

3. Model

3.1 "Collection of Point Dipoles" Model

Associated with the vehicle are N point dipoles with dipole moments $\vec{m}_i$, $i = 1, \ldots, N$, located at the points $\vec{x}_i'$ fixed in the vehicle. As the vehicle passes a three-axis magnetometer located at position $\vec{x}_0$ in frame S (or equivalently, at $\vec{x}_0'(t) = \vec{x}_0 - \vec{v}t$ in S'), the sensor registers a time-dependent magnetic flux density (B-field) that is the superposition of their individual dipole fields:

$$\vec{B}(t) = \frac{\mu_0}{4\pi} \sum_{i=1}^{N} \left[\frac{3\big(\vec{m}_i \cdot \vec{r}_{i0}(t)\big)\, \vec{r}_{i0}(t)}{|\vec{r}_{i0}(t)|^5} - \frac{\vec{m}_i}{|\vec{r}_{i0}(t)|^3} \right]. \tag{8}$$

Here, μ_0 is the permeability of free space, with a measured value equal to the previously defined value of $4\pi \times 10^{-7}$ T m/A to within experimental uncertainty, and

$$\vec{r}_{i0}(t) = \vec{x}_0'(t) - \vec{x}_i' = \vec{x}_0 - \vec{v}t - \vec{x}_i' \tag{9}$$

is the vector from the ith dipole to the observation point (sensor); it is represented in Figure 2 by the blue, dashed arrow. Note that whereas $\vec{x}_0$ and $\vec{x}_0'(t)$, the position vectors of the sensor in the S and S' frames, respectively, lie in the xy-plane, both $\vec{r}_{i0}(t)$ and the dipole position vectors $\vec{x}_i'$ have a z-component, and this vertical component is not indicated in Figure 2; rather, in the "top view" shown in Figure 2, $\vec{r}_{i0}(0)$ and $\vec{x}_i'$ are represented by their projections in the xy-plane.

We express the time dependence of $\vec{r}_{i0}(t)$ and $\vec{x}_0'(t)$ explicitly to emphasize that in S', the sensor moves "backwards" with velocity $-\vec{v}$. This observation suggests an alternative—and somewhat more general—means of expressing our results: instead of associating values of the magnetic field with the time t at which they are recorded by the sensor, we can associate them with the position $\vec{x}_0'(t)$ in S' at which the sensor is located when the measurement is made, or even, for a fixed path traversed in S' by the sensor, by the coordinate $s = vt$ related to the distance traveled by the sensor along that path. The point is that a plot of magnetic flux density versus the distance coordinate s defined by the latter prescription is independent of the speed of the vehicle, whereas a plot of magnetic flux density versus the time coordinate t given by the former prescription is not.

3.2 Far-Field Approximation: Single-Dipole Asymptotic Model

In most sensing scenarios involving a ground vehicle, the distance $x_0'(t)$ between the sensor and the vehicle always far exceeds the maximum dimension L of the vehicle: its "length." In this section, we develop an approximate expression for the B-field recorded by the sensor in this case.

Since all the dipoles associated with the vehicle must lie within it, $x_i' \leq L$ for all $i = 1, \ldots, N$. The distance between sensor and vehicle, $x_0'(t)$, is bounded from below by the distance of closest approach: $x_0'(t) \geq d_{CPA}$. We define the small parameter

$$\delta \stackrel{\text{def}}{=} \frac{x_i'}{x_0'(t)} \leq \frac{L}{d_{CPA}} \ll 1 \,, \tag{10}$$

and we express the vector from the ith dipole to the sensor as

$$\vec{r}_{i0}(t) = x_0'(t)\left(\hat{x}_0'(t) - \frac{\vec{x}_i'}{x_0'(t)}\right) = x_0'(t)(\hat{x}_0'(t) - \delta\,\hat{x}_i')\,, \tag{11}$$

with magnitude

$$r_{i0}(t) = x_0'(t)\left[1 - \frac{\hat{x}_0'(t)\cdot\vec{x}_i'}{x_0'(t)} + O(\delta^2)\right] = x_0'(t)[1 - \delta\,(\hat{x}_0'(t)\cdot\hat{x}_i') + O(\delta^2)] \tag{12}$$

Here, $\hat{x}_0'(t)$ and $\hat{x}_i'$ are unit vectors in the direction of the position $\vec{x}_0'(t)$ of the sensor and of the position $\vec{x}_i'$ of the ith dipole, respectively, both with respect to the moving frame S'. Expanding the expression for the summands on the right-hand side of Equation 8, we obtain

$$\begin{aligned}\vec{B}(t) \;=\; \frac{\mu_0}{4\pi x_0'^3}\textstyle\sum_{i=1}^{N}\{[3(\vec{m}_i\cdot\hat{x}_0')\,\hat{x}_0' - \vec{m}_i\,] - \\ 3\delta\,[(\vec{m}_i\cdot\hat{x}_i')\,\hat{x}_0' + (\vec{m}_i\cdot\hat{x}_0')\,\hat{x}_i' - (\hat{x}_0'\cdot\hat{x}_i')\,\vec{m}_i + 5(\vec{m}_i\cdot\hat{x}_0')(\hat{x}_0'\cdot\hat{x}_i')\,\hat{x}_0'] \\ +\; O(\delta^2)\}\end{aligned} \tag{13}$$

so to leading order in δ,

$$\vec{B}(t) = \frac{\mu_0}{4\pi}\frac{3\left(\vec{m}\cdot\hat{x}_0'(t)\right)\hat{x}_0'(t) - \vec{m}}{\left[x_0'(t)\right]^3}\,, \tag{14}$$

where

$$\vec{m} = \textstyle\sum_{i=1}^{N}\vec{m}_i\,. \tag{15}$$

Thus, we see that if the distance of closest approach of the vehicle to the sensor far exceeds the vehicle length, the B-field recorded by the sensor is that of a single point dipole situated at the origin of the moving frame S', and the dipole moment of this equivalent point dipole is given by the vector sum of the individual point dipoles in the original model. Observe that we have chosen the origin of S' to lie at the point on the ground directly below the center of the vehicle, whereas all the individual dipoles lie at some height above the ground; in other words, each dipole position $\vec{x}_i'$ has a positive z-component h_i. However, since $\hat{x}_0'(t)$ lies in the xy-plane, the z-component of $\hat{x}_i'$ does not contribute to the dot product that appears in the term on the right-hand side of Equation 12 that is first order in δ. The impact of the z-component of each $\vec{x}_i'$ only is $O(\delta^2)$, and the error made by replacing the "slant line distance" $r_{i0}(t)$ by its projection on the plane of the ground is negligible for $r_{i0}(t) \gg L \geq h_i$.

3.3 Anderson Function Representation

We proceed by way of the elegant representation originally developed by J.E. Anderson in the 1940s to efficiently calculate the magnetic anomaly resulting from submarine moving relative to a ship-based sensor.[5,6] The submarine is represented as a single magnetic dipole located at the origin of the frame S'. In this formalism, the time dependence is carried by the three Anderson functions

$$f_n(\theta) \stackrel{\text{def}}{=} \frac{\theta^n}{[1+\theta^2]^{5/2}}\,, \; n \in \{0, 1, 2\}\,, \tag{16}$$

which depend on the dimensionless parameter

$$\theta = \frac{vt}{d_{CPA}} = \frac{s}{d_{CPA}}\,. \tag{17}$$

In the latter equality, s, introduced above in Section 3.1, is the coordinate along the path traversed by the sensor when viewed from the moving frame S'.

The magnetic anomaly resulting from a single dipole of moment $\vec{m}$ located at the origin in S' is

$$\vec{B}(\theta) = \frac{\mu_0}{4\pi d_{CPA}^3} \sum_{n=0}^{2} f_n(\theta)\, \mathbf{A}_n(\alpha) \cdot \vec{m}\;, \tag{18}$$

where $\mathbf{A}_n(\alpha)$, $n = 0, 1, 2$, is constant, second-rank tensor that depends only on the geometry of the encounter, which is completely specified by the azimuth α of the vehicle. The three tensors may be represented by three traceless 3 × 3 symmetric matrices that multiply the column vector $\vec{m}$ by ordinary matrix multiplication:

$$\mathbf{A}_0(\alpha) = \begin{pmatrix} 3\cos^2(\alpha) - 1 & -3\cos(\alpha)\sin(\alpha) & 0 \\ -3\cos(\alpha)\sin(\alpha) & 3\sin^2(\alpha) - 1 & 0 \\ 0 & 0 & -1 \end{pmatrix}, \tag{19}$$

$$\mathbf{A}_1(\alpha) = 3\sigma \begin{pmatrix} -\sin(2\alpha) & -\cos(2\alpha) & 0 \\ -\cos(2\alpha) & \sin(2\alpha) & 0 \\ 0 & 0 & 0 \end{pmatrix}, \tag{20}$$

$$\mathbf{A}_2(\alpha) = \begin{pmatrix} 3\sin^2(\alpha) - 1 & 3\cos(\alpha)\sin(\alpha) & 0 \\ 3\cos(\alpha)\sin(\alpha) & 3\cos^2(\alpha) - 1 & 0 \\ 0 & 0 & -1 \end{pmatrix}, \tag{21}$$

We observe that $\mathbf{A}_n(\alpha) = \mathbf{A}_n(\alpha + \pi)$ for $n = 0, 1, 2$.

Equation 18 shows how the magnetic anomaly registered by the sensor may be expressed as the sum of three terms, each of which is the product of a factor carrying the time or distance dependence, a constant factor related to the geometry of the encounter between the sensor and the magnetic source, and the magnetic moment of the dipole.

4. Procedure for Estimating Kinematic Parameters

Equations 17–21 provide a method for obtaining estimates of selected parameters related to the movement of a ground vehicle from time series data of the magnetic anomaly resulting from the vehicle. From the vertical (z-) component of the magnetic anomaly data, we first obtain an estimate of the ratio v/d_{CPA} of the vehicle speed to the distance of closest approach of the vehicle to the sensor. The value of this ratio is then used to determine the direction of vehicle travel (azimuth angle α) modulo 180° from the components of the anomaly data in the horizontal (xy-) plane. Along the way, we also determine the values of three additional parameters related to the three components of the dipole moment of the vehicle:

$$\vec{b} \stackrel{\text{def}}{=} \frac{\mu_0}{4\pi d_{CPA}^3} \vec{m}\,, \tag{22}$$

but we will make no use of these. The parameters $\vec{b}$ carry the same physical units as the magnetic flux density: tesla (SI) or gauss (cgs).

The formidable appearance of Equation 18 notwithstanding, the z-component of the magnetic anomaly has a surprisingly simple form:

$$B_z(\theta) = \frac{b_z}{[1+\theta^2]^{3/2}}\,, \tag{23}$$

where b_z is defined in Equation 22 and the dimensionless "time" parameter $\theta = (v/d_{CPA})\, t$ by Equation 17. Physically, b_z is the magnetic flux density measured by the magnetometer when the vehicle is at its CPA. The maximum value of $B_z(t)$ over the time series provides a preliminary estimate of b_z, which is used as a starting value in a two-parameter nonlinear fit of the time series. This fit yields a final value of b_z as well as the value of the ratio v/d_{CPA}. Observe that the inverse ratio $d_{CPA}/v \stackrel{\text{def}}{=} \tau$ defines the characteristic time scale for the time series.

The expressions obtained from Equation 18 for $B_x(\theta)$ and $B_y(\theta)$, the components of the magnetic anomaly in the horizontal plane, are more complicated. Writing s and c for $\sin(\alpha)$ and $\cos(\alpha)$, respectively, and applying well-known trigonometric identities, we have

$$B_x(\theta) = [1+\theta^2]^{-5/2} \begin{Bmatrix} \left[(3c^2-1)b_x - 3csb_y\right] + \\ \sigma\theta\left[-6csb_x - 3(c^2-s^2)b_y\right] + \\ \theta^2\left[(3s^2-1)b_x + 3csb_y\right] \end{Bmatrix} \tag{24}$$

$$B_y(\theta) = [1+\theta^2]^{-5/2} \begin{Bmatrix} \left[-3csb_x + (3s^2-1)b_y\right] + \\ \sigma\theta\left[-3(c^2-s^2)b_x + 6csb_y\right] + \\ \theta^2\left[3csb_x + (3c^2-1)b_y\right] \end{Bmatrix}. \tag{25}$$

The estimate of v/d_{CPA} obtained by fitting Equation 23 to the z-component of the anomaly time series data is used to convert the independent variable of the x- and y-components of the anomaly data from t (time) to θ, and the resulting "theta series" are fit to determine the unknown parameters b_x, b_y, and α using a two-step, nested procedure. A 1D line search for α is performed, with the value of the "sum of squared residuals" objective function for each value of α determined by a two-parameter, linear least-squares fit for b_x and b_y. To avoid issues with critical points that do not correspond to the global minimum of the objective function, the search for α is performed over the extended range $-(\pi+\varepsilon) < \alpha < \pi + \varepsilon$, where $\varepsilon > 0$ is small real parameter. If necessary, the optimal value of α is translated back into the range $0 \le \alpha < \pi$ at the conclusion of the procedure.

5. Representative Results

In this section, we employ the methodology described above to estimate a ground vehicle's direction of travel (azimuth angle α) modulo 180° and the value of the ratio v/d_{CPA} of the vehicle's speed to its distance of closest approach to the sensor. For this purpose, we utilize simulated data sets for which the quantities v, d_{CPA}, and α are precisely known, in contrast to data obtained in a field test, where there is always some uncertainty in both v and d_{CPA} and where the sensor may not be situated sufficiently far from the path of the vehicle to ensure validity of the far-field assumption ($d_{CPA} \gg L$) implicit in the model.

5.1 Single Dipole: Passenger Car

Figure 3 shows the results obtained from simulated magnetic anomaly data for a typical passenger automobile, modeled as a single induced point dipole situated at the origin of the moving frame S' and passing a magnetic field sensor at a closest-approach distance d_{CPA} of 5 m. In this case, the assumption that the data represent a single dipole is exact, valid for all values of d_{CPA}, and not merely true asymptotically at closest-approach distances that are large compared to the dimensions of the vehicle. In Figure 3a, the vehicle is traveling 15° north of due east (azimuth 75°) at 10 mph (4.5 m/s); in Figure 3b, it is traveling due east (azimuth 90°) at 25 mph (11.2 m/s); and in Figure 3c, it is traveling 15° west of due north (azimuth 345°) at 25 mph.

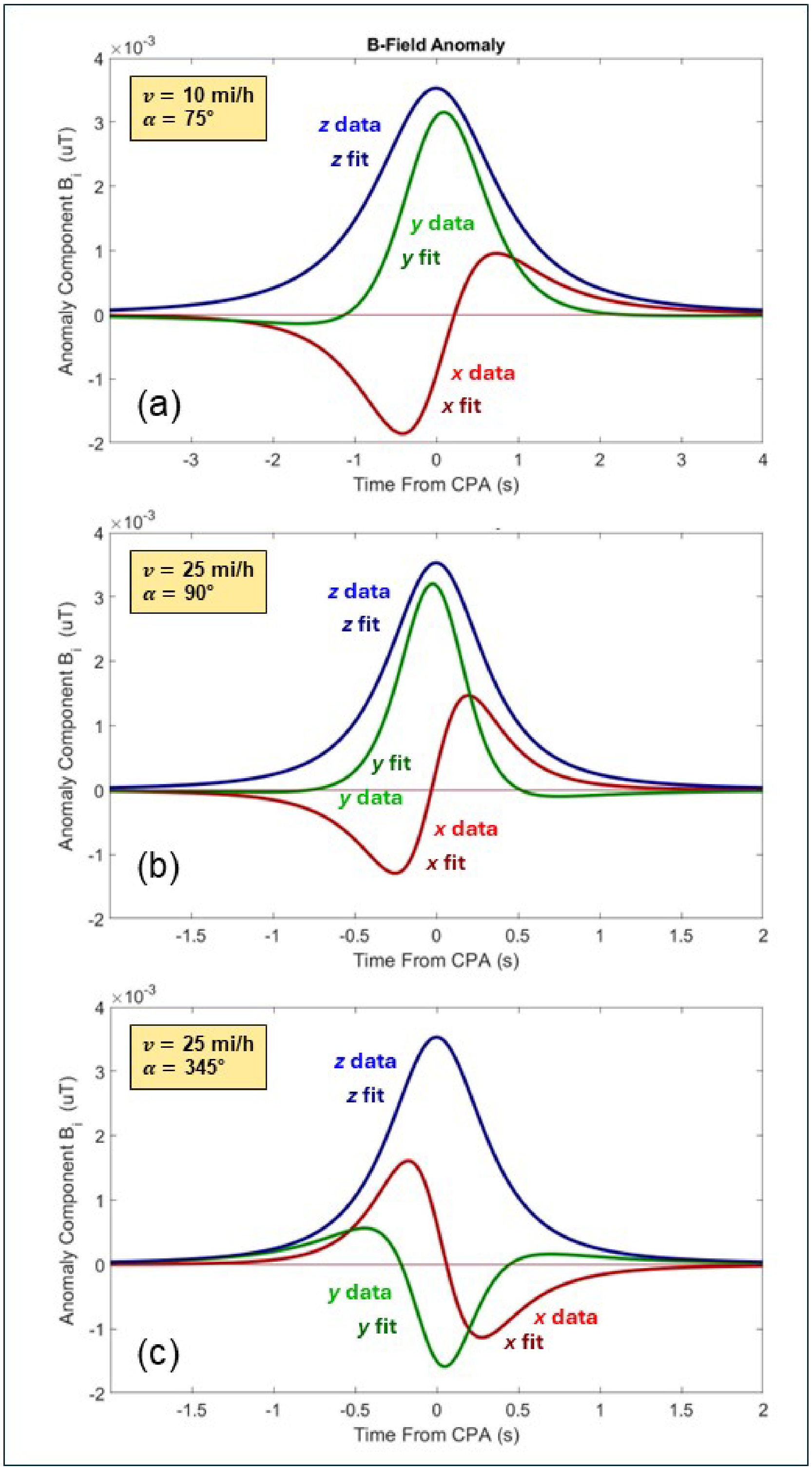

Figure 3. **(a–c) Components of the simulated magnetic anomaly of a passenger automobile traveling with azimuth α and speed v past a magnetometer at $d_{CPA} = 5$ m (brighter hues) with fits used to estimate α modulo 180° and the ratio v/d_{CPA} from the data (darker hues).**

The x-, y-, and z-components of the magnetic anomaly registered by the sensor as a function of time are represented in Figure 3 by the curves in the brighter shades of red, green, and blue, respectively, whereas the fits used to estimate v/d_{CPA} and α are represented by curves in darker shades of their respective hues. The former curves are seen to coincide almost perfectly with the latter, and the procedure described in Section 4 precisely determines the values of the parameters v/d_{CPA} and α (as well as the values of b_x, b_y, and b_z, which we do not use directly). The only exception to this occurs with the simulated data displayed in Figure 3c, where the procedure yields an estimated azimuth angle of 165°, instead of the true value of 345°. This illustrates one of the principal deficiencies of the model: using data from only a single magnetometer, one cannot determine in which of two diametrically opposed directions the vehicle is traveling; that is, azimuths of α and $\alpha + \pi$ are indistinguishable. However, this ambiguity is easily removed using data from a second sensor, either a nearby magnetometer or an acoustic sensor, possibly collocated with the first magnetometer.

5.2 Multiple Dipoles: Tank

We now examine a more complicated example that illustrates the difficulties that can arise if the far-field assumption is not satisfied. We model the magnetic anomaly of a main battle tank as a collection of four induced point dipoles associated physically with the front hull and turret armor, the rear hull and turret armor, the engine, and the remaining automotive components. Open literature sources give the length, width, height, and ground clearance of the vehicle as 7.05, 3.89, 2.73, and 0.49 m, respectively. We take the dipoles to be situated along the center line of the vehicle at various heights above the ground, and we assume that it travels due east (true azimuth $\alpha = 90°$) at 25 mph.

Table 1 assembles the estimates and ground truth values of v/d_{CPA} and α for various values of d_{CPA}, the distance of closest approach of the vehicle to the sensor: 5, 10, and 20 m. In addition, Table 1 provides the minimum value of SSE, the sum of squared residuals in the fit of the horizontal anomaly components used to obtain the estimate of α. Figure 4 displays the x-, y-, and z-components of the simulated magnetic anomaly data corresponding to the closest-approach distances in Table 1, together with plots of the single-dipole fits used to determine the parameter estimates appearing in the table. The color scheme used to identify the various curves in Figure 4 is identical to that used in Figure 3.

Table 1. Kinematic parameters derived from simulated magnetic anomaly data of a tank.

d_{CPA}		5 m	10 m	20 m
Estimated v/d_{CPA}	s^{-1}	1.99	1.11	0.57
True v/d_{CPA}	s^{-1}	2.24	1.12	0.56
Estimated azimuth α	deg	14	85	90
True azimuth α	deg	90	90	90
SSE	nT^2	3650	125	0.422

It is clear from Table 1 that unless the sensor is situated at least one vehicle length (and ideally, several vehicle lengths) from the path of the passing vehicle, the estimates of v/d_{CPA} and α obtained from the procedure of Section 4 may be inaccurate.

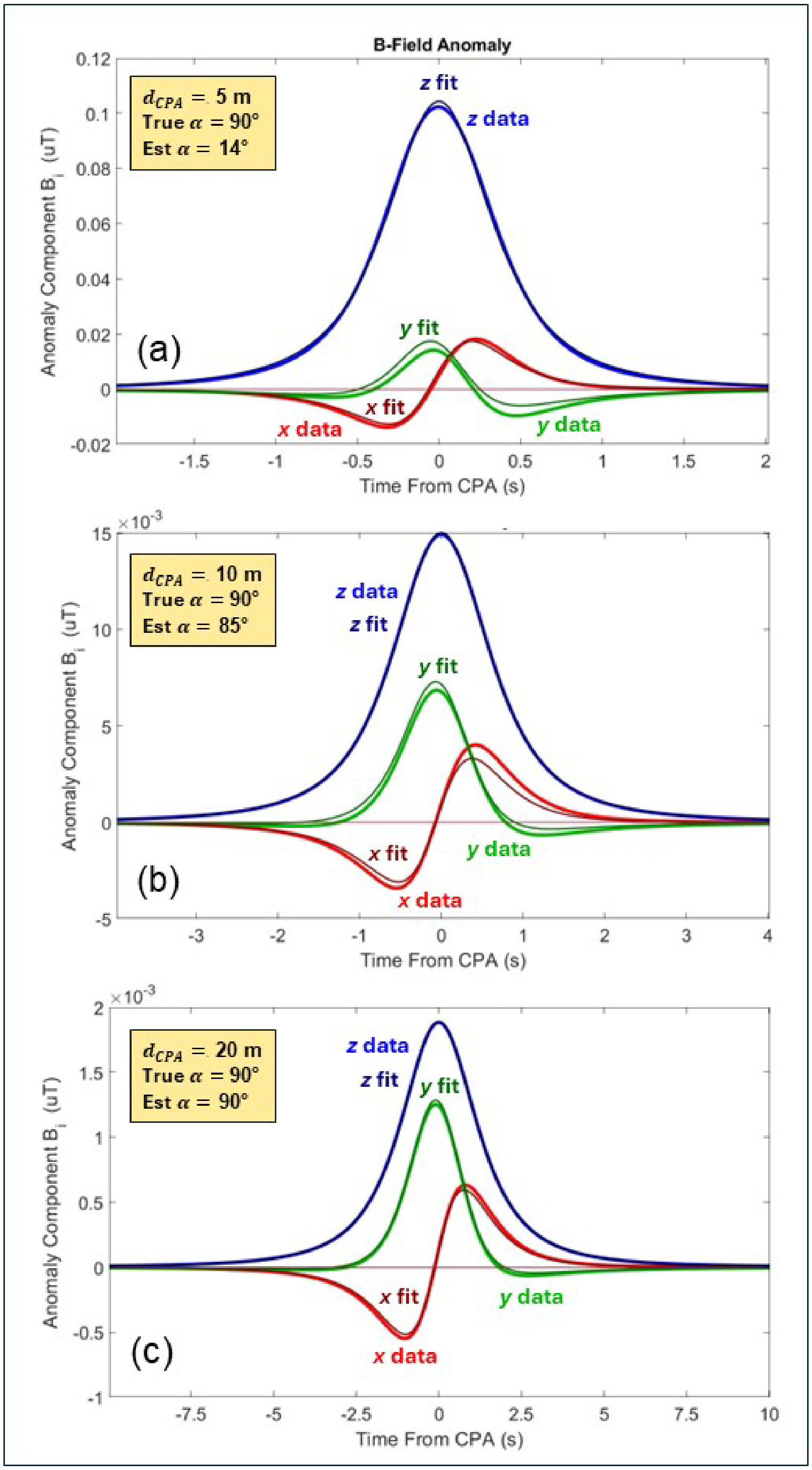

Figure 4. (a–c) Components of the simulated magnetic anomaly of a tank traveling 25 mph eastward past a sensor at various distances d_{CPA} of closest approach (brighter hues) with fits used to estimate α modulo 180° and the ratio v/d_{CPA} from the data (darker hues).

5.3 Effect of Random Noise: Tank

The preceding examples demonstrate that as long as the target vehicle is sufficiently far from the sensor (multiple vehicle lengths at CPA), the procedure described in Section 4 accurately estimates the ratio v/d_{CPA} and the azimuth angle α modulo 180°—at least when it is applied to smooth, simulated data. The simulated data in Figure 5 were obtained from those in Figure 4c by the addition of $N(0,\sigma)$-distributed white noise, where $\sigma = 0.1b_z = 0.19$ nT. Applied to these noisy data, the procedure continues to provide accurate estimates of v/d_{CPA} and α. The presence of noise in the data is reflected in SSE, the minimum value of the objective function used to simultaneously fit the horizontal components of the simulated data and obtain the least-squares estimate of α: 71.3 nT^2 for the fits in Figure 5, versus 0.422 nT^2 for those in Figure 4c. The color scheme used to identify the various curves in Figure 5 is the same as that used in Figures 3 and 4.

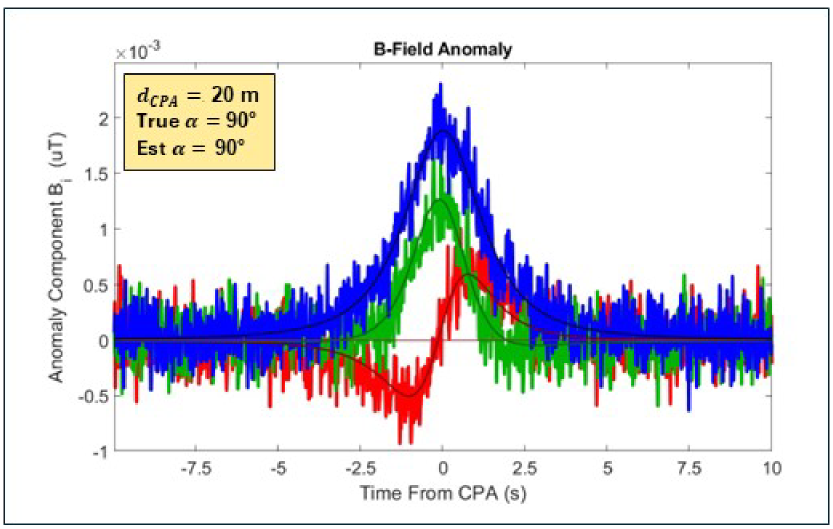

Figure 5. Jagged red, green, and blue lines indicate the x-, y-, and z-components, respectively, of the simulated magnetic anomaly of a tank traveling 25 mph eastward past a sensor at d_{CPA} = 20 m. The simulated anomaly data include additive Gaussian white noise. The smooth lines in darker shades of their respective hues indicate the corresponding fits used to estimate α modulo 180° and the ratio v/d_{CPA} from the data.

6. Conclusion

We consider the case of a small, low-cost unattended ground sensor (UGS) emplaced in an area in which surveillance is desired. In the most common sensor emplacement scenario, the UGS will be deployed along a roadway at a relatively low density. To make the UGS less conspicuous to drivers of passing vehicles and to avoid roadside features (e.g., drainage ditches) that might impair sensor function, the UGS will ideally be emplaced near—but not precisely at the side of—a road. Thus, it is likely that most sensors will be sufficiently distant from the passing vehicles that the far-field approximation is valid and the estimates of v/d_{CPA} and α provided by the model are accurate, even in the presence of significant noise.

The magnetic anomaly due to an object varies as the inverse cube of the distance between the object and the observation point. This fundamental physical fact, in combination with the limited sensitivity of low size, weight, and power magnetic field sensors, sets the upper bound on a window of CPA distances at which sensors should be deployed for the methods described here to be successfully applied: d_{CPA} must be large enough (at least one—ideally several— vehicle lengths) for the far-field assumption of the model to be valid, but not so large that the signal recorded by the magnetometer is completely lost in noise.

Of course, in the presence of a roadway, the ability to determine a vehicle's direction of travel modulo 180° in general provides little marginal utility, since in virtually all cases the vehicle will travel on the road, and its azimuth modulo 180° is simply that of the road itself and can be determined from a map. That said, reliable indications that a vehicle is *not* proceeding along an existing road, but rather is traveling off-road in a different direction, could represent extremely high-information-value intelligence indeed.

It may be that the kinematic parameters derived from magnetic anomaly time series data by the methods described here will prove to be most useful in corroborating estimates obtained using other sensor modalities (e.g., acoustic). Provided certain conditions are met, these parameter estimates are quite accurate, and the magnetic anomaly measurements on which they are based are virtually impervious to spoofing.

7. References

1. Pritchett TM, Canady AT Jr, Vinci SJ. Modeling magnetic signatures of tactical ground vehicles using the boundary element method. Proceedings of the 2024 Military Sensing Symposium on Battlefield Acoustic, Seismic, Magnetic, and Electric Field Sensors (MSS-BAMS); 2024 Oct 28–Nov 1; Laurel, MD; 2024. Paper No.: B5A01.

2. Sheinker A, Frumkis L, Ginzburg B, Salomonski N, Kaplan B-Z. Magnetic anomaly detection using a three-axis magnetometer. IEEE Trans Magn. 2009;45(1):160–167. https://doi.org/10.1109/TMAG.2008.2006635

3. Yan Y, Liu J, Yan S, Shen S, Li X. An effective magnetic anomaly detection using orthonormal basis of magnetic gradient tensor invariants. IEEE Trans Geosci Remote Sens. 2024;62:2001611. https://doi.org/10.1109/TGRS.2024.3353303

4. Lenz J, Edelstein S. Magnetic sensors and their applications. IEEE Sens J. 2006;6(3):631–649. https://doi.org/10.1109/JSEN.2006.874493

5. Loane EP. Speed and depth effects in magnetic anomaly detection. EPL Analysis; Ashton, MD; 1976.

6. Wynn WM. Detection, localization, and characterization of static-dipole sources. In: Baum CE, editor. Detection and identification of visually obscured targets. Routledge; 1998. Chapter 11, p. 337–374.

List of Symbols, Abbreviations, and Acronyms

1D	one-dimensional
CPA	closest point of approach
UGS	unattended ground sensors

1 DEFENSE TECHNICAL
(PDF) INFORMATION CTR
DTIC OCA

1 DEVCOM ARL
(PDF) FCDD RLB CI
TECH LIB